PERFORMANCE OF FACTORY MADE SOLAR HEATING SYSTEMS ACCORDING TO STANDARD ISO 9459-5:2007

Vera-Medina, J.[1], Larrañeta M[2], Lillo-Bravo,I.[2]

[1] Solar Thermal Energy Department, National Renewable Energy Centre (CENER)

[2] Department of Energy Engineering, University of Seville.

Corresponding author:

Jonathan Vera. National Renewable Energy Centre (CENER), C/ Isaac Newton, Nº4. Pabellón de Italia, 5ª Planta SO, 41092, Seville, Spain.

Phone number: (+34)948252800

E-mail: jvera@cener.com

Highlights

Abstract

The utilization of solar energy based technologies has attracted increased interest in recent times in order to satisfy the energy demands in buildings. This research work presents a comparative analysis of the energy production and costs of factory made solar heating systems, Thermosiphon Solar Water Heaters Systems (TSWHS) and Forced-circulation Solar Water Heaters Systems (FSWHS), as a function of profile type (high and low) and collector absorber treatment (selective and black painting). We observe that the energy performance and the Levelized Cost of Energy (LCOE) is similar in TSWHS and FSWHS for load volumes below tank nominal volume, black painting absorbers and locations with high solar irradiation. In the case of load volumes greater than nominal, climates with low irradiation and collectors with selective absorbers, the differences in their energy performance can reach a 7% and the LCOE can increase up to 9%. The LCOE is lower for TSWHS systems for all the evaluated scenarios. We have also found that for cold climates, the FSWHS systems present higher net annual energy produced, however, for warm climates TSWHS systems present greater net annual energy production.

Keywords: Solar system, performance, testing, profile.

1. - Introduction

Building sector is experiencing significant challenges in relation to greenhouse gas emissions, energy consumption and associated costs. These changes are mainly due to a legislative change [1], long-term trend of increasing energy prices [2] and emerging market of renewable energy [3].

A legal frame is already formulated in European Union. Directive 2010/31/EU [4] states the implementation of Nearly Zero-Energy Buildings (NZEBs) starting with 2019 for new public buildings and by 2021 for any new building, amended by the Directive (EU) 2018/844 [5] establishing that each member state shall have a long-term renovation strategy to support the renovation of the stock of buildings, into a highly energy efficient and decarbonised building stock by 2050, reducing greenhouse gas emissions in the Union by 80-95 % compared to 1990. The roadmap shall include indicative milestones for 2030, 2040 and 2050, and specify how they contribute to achieving the Union's energy efficiency targets in accordance with Directive 2012/27/EU, [6] facilitating the cost-effective transformation of existing buildings into nearly zero-energy buildings.

Building-Integrated Solar Thermal (BIST) systems are a new tendency in the building sector, which tries to benefit from the synergy of refurbishing the building and installing solar thermal collectors at the same time with a significant visual comfort [7]. There are a variety of solutions in BIST systems, all of them designed as they allow the use of solar collectors that, in addition to energy production, have other functions within the building, such as daylighting, glare control, solar control, air tightness, safety in case of fire, protection against noise, [8]. There are many ongoing efforts to improve these solutions. The IEA SHC Task 56 is a global activity focused on Building Integrated Solar Envelope Systems for HVAC and Lighting. It is centered on the analysis of multifunctional envelopes that use or control incident solar energy in order to deliver renewable thermal energy to the buildings [9]. In addition, there are already solutions in the market for building-added solar thermal collectors in roofs and facades [10] such as the integration of solar collectors as shading devices according to aesthetic considerations [11] or all-ceramic solar collectors [12] [13]. There are specialized companies such as SIKO SOLAR GmbH focused in building integration: basic and classic. As an example, the Sun House and KOMBISOL house in Austria [14]. There are also manufacturers like DOMMA Solartechnick GmbH that offer custom-made flat-plate BIST collectors [15].

This new trend is an alternative of Factory made solar heating systems are compact, very reliable, efficient and durable since all the equipment of the solar installation are designed and tested before installation to verify their specifications with the test standards. For example, on the European market must overcome the EN 12976:2017 [16] [17] European Standard tests. The European Standard efficiency test refers to two ISO Standards, ISO 9459-2:2008 [8] and ISO 9459-5:2007 [19]. On the USA market must overcome the ICC_900-SRCC 300:2015 Standard tests [20].

There are two main configurations of Factory Made Solar Heating Systems in the market: Thermosiphon Solar Water Heaters Systems (TSWHS) and Forced-circulation Solar Water Heaters Systems (FSWHS).

FSWHS need additional equipment such as sensors, a controller and a pump. Moreover, its cost is greater than TSWHS. FSWHS systems present the possibility of locating the water storage tank inside the house; reducing its thermal losses, besides, their visual impact is much lower than the TSWHS, since the solar collectors can be adapted to the building envelope being a solution that can be used for BIST applications. Moreover, FSWHS can incorporate in the control system two protection mechanisms: frost protection and overheating protection.

TSWHS are the simplest and most widely used solar energy collection and utilization devices particularly in countries with high sunshine potential [21]. They are more reliable, and have a longer life than forced circulation systems. Moreover, they do not require an electrical supply to operate and they naturally modulate the circulation flow rate, which is in phase with the irradiation levels. However, the visual impact of TSWHS is high because the storage tank in TSWHS has to be mounted above the collectors in order to promote the thermosiphon flow and to avoid the reverse circulation of the working liquid when the temperature of the collector is lower than the temperature of the storage tank, normally during night. The relative height separating the tank and collector mainly influences the magnitudes of the thermosiphon flow rates, including both forward and reverse flow at night [22].

Morrison et al [23] found that the TSWHS performance is maximized when the daily collector volume flow is approximately equal to the daily load flow, and that TSWHS with vertical tank present better performance than TSWHS with horizontal tank. Nevertheless, tanks on vertical position have more visual impact than tanks on horizontal position and therefore horizontal tanks are more frequently used. Sotaris et al [24] investigated possible configurations of the TSWHS with the Typical Meteorological Year of Nicosia, Cyprus. They found that the distance between the top of the collector and the bottom of the storage tank affects the performance of the system. The smaller this distance is, the higher the system performance, which is also beneficial for the esthetical improvement of the system. Bo et al [25] analyzed the pros and cons of replacing traditional materials with polymeric materials in TSWHS. They highlight that polymeric materials can increase the climatic and environmental performance of the thermosiphon system and reduce their total cost of energy. An option to reduce the visual impact of conventional TSWHS is to place the solar tank hidden behind the solar collector as it happens with low profile TSWHS [26],[27].

The aim of this paper is compare the thermal performance and LCOE of different factory made solar heating systems under different climatic conditions (Athens, Davos, Stockholm and Wurzburg) and different daily load volumes, according to the Standard ISO 9459-5:2007 [19].

In particular, we have compared two factory made High profile TSWHS, two factory made Low profile TSWHS and two factory made FSWHS with two types of flat-plate solar collector, one of low emissivity and another of black painting. All Solar Water Heaters Systems (SWHS) have identical collector size and solar tank volume.

With the obtained results, we have a quantification of the energy and economic differences of the different configurations as a function of the climate. This quantification can be used for the selection criterion between factory made solar heating systems and as a reference for the BIST systems.

The paper is presented as follows: In Section 2 we describe the solar systems and the testing method. Section 3 shows the main experimental results and the techno-economic analysis. Conclusions are then made in Section 4.

2. Methodology

This section includes the description of the tested factory made solar heating systems and the testing method description.

2.1- Description of tested factory made solar heating systems.

Six factory made solar heating systems of identical collector sizes and solar tank volume have been tested. Four systems are TSWHS types and two systems are FSWHS. In table 1 we present the main technical characteristics of each tested unit according to the manufacturer and verified in our laboratory. All systems are from the same manufacturer. Six systems have flat-plate solar collectors with the following differences:

T-High-LowE: High profile TSWHS with low emissivity absorber.

T-Low-LowE: Low profile TSWHS with low emissivity absorber.

F-LowE: FSWHS with low emissivity absorber.

T-High-Black: High profile TSWHS with black painting absorber.

T-Low-Black: Low profile TSWHS with black painting absorber.

F-Black: FSWHS with black painting absorber.

Table 1- Constructive parameters of the six tested systems. The numbers in parentheses refer to the components shown in figures 1, 2 and 3.

System parameters	T-High-LowE	T-Low-LowE	F-LowE	T-High-Black	T-Low-Black	F-Black	Unit
System type	Thermosiphon	Thermosiphon	Forced-circulation	Thermosiphon	Thermosiphon	Forced-circulation	--
Profile type	High profile	Low profile	--	High profile	Low profile	--	--
Surface treatment of the absorbers	Mirotherm Selective	Mirotherm Selective	Mirotherm Selective	Black painting	Black painting	Black painting	--
Absorber absorption coefficient.	0.95	0.95	0.95	0.98	0.98	0.98	%
Absorber emissivity coefficient to 100ºC	0.05 ± 0.01	0.05 ± 0.01	0.05 ± 0.01	0.94	0.94	0.94	%
Aperture area of the collector	2.58	2.58	2.58	2.58	2.58	2.58	m^2
Tank volume	200	200	200	200	200	200	litres
Tank position respect to collector	Above	Behind	Indoor Storage	Above	Behind	Indoor Storage	--
Collector array tilt	45	45	45	45	45	45	º
Reverse flow protection valve of consumer loop (1)	Yes	Yes	Yes	Yes	Yes	Yes	--
Safety valve of consumer loop (2)	Yes	Yes	Yes	Yes	Yes	Yes	--
Safety valve of solar loop (3)	Yes	Yes	Yes	Yes	Yes	Yes	--
Heat transfer fluid	Water+ glycol (20 %)	Water+ glycol (20 %)	Water+ glycol (20 %)	Water+ glycol (20 %)	Water+ glycol (20 %)	Water+ glycol (20 %)	--
Auxiliary Energy	No	No	No	No	No	No	
Reverse flow protection valve of solar loop (4)	No	Yes	Yes	No	Yes	Yes	--
Expansion vessels volume (5)	--	8	8	--	8	8	litres
Manometer (6)	No	Yes	Yes	No	Yes	Yes	--
Drain valve (7)	No	Yes	Yes	No	Yes	Yes	--
Pump (8)	No	No	Yes	No	No	Yes	--
Controller (9)	No	No	Yes	No	No	Yes	--
Fill closed loop	Atmospheric	1.5	1.5	Atmospheric	1.5	1.5	bar

Figure 1 shows a picture and the connection scheme for the high profile TSWHS (Systems T-High-LowE and T-High-Black). Figure 2 shows a picture and the connection scheme for the low profile TSWHS (T-Low-LowE and T-Low-Black) and Figure 3 shows a picture and the connection scheme for FSWHS (F-LowE and F-Black). The main difference between the TSWHS presented in Figure 1 and 2 is that low profile TSWHS must include several elements to avoid reverse flow increasing their cost and reducing its energy performance. These elements are an expansion vessel, a reverse flow protection valve and a pressurized solar loop.

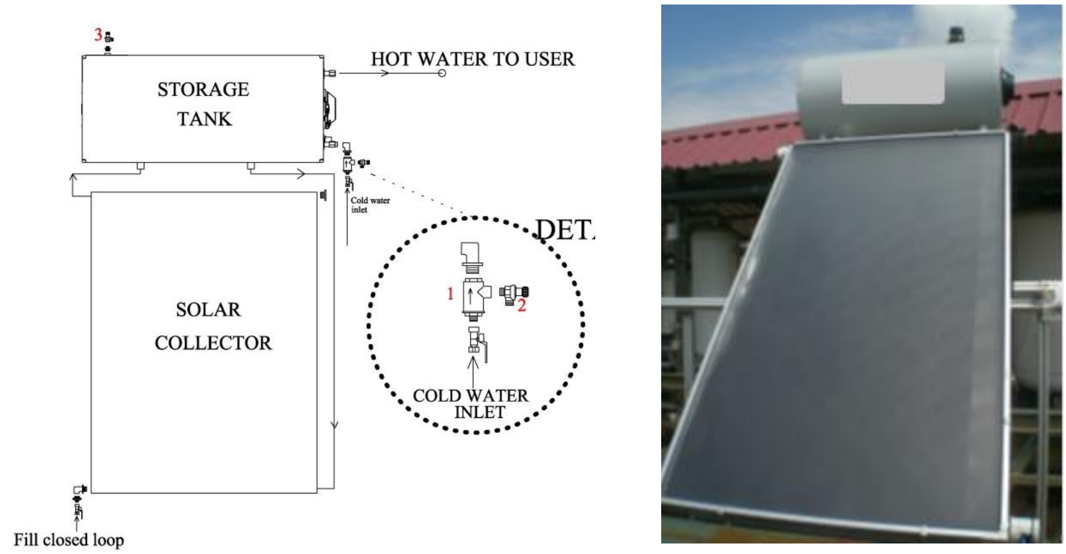

Fig 1. Schematic diagram of high profile TSWHS.

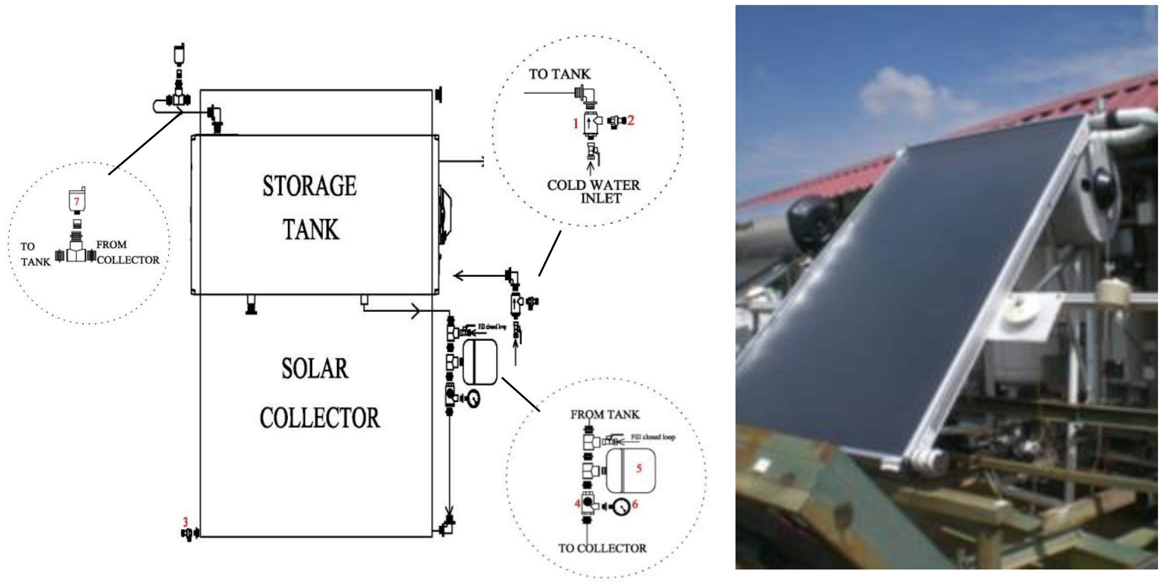

Fig 2. Schematic diagram of low profile TSWHS

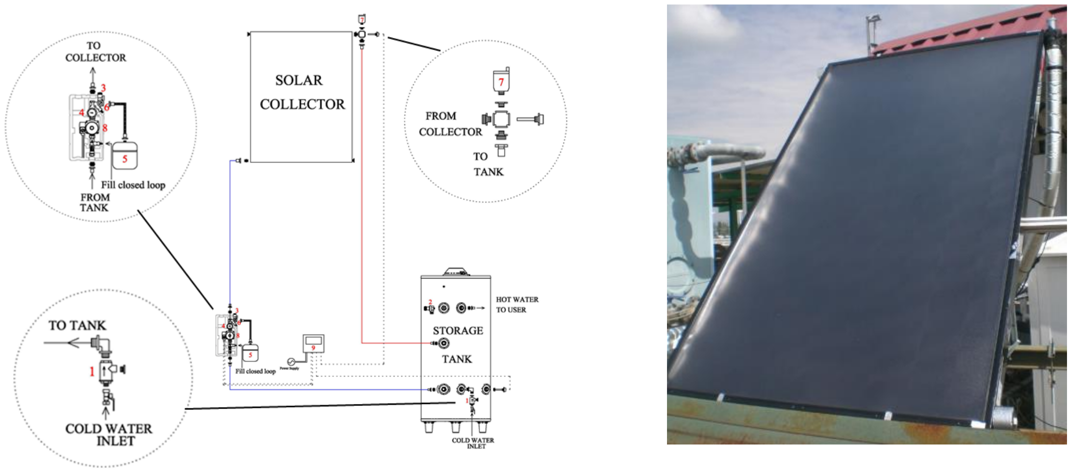

Fig 3. Schematic diagram of FSWHS

2.2. - Testing method description

Six factory made solar heating systems have been tested according to the Standard ISO 9459-5:2007 [19] in the accredited solar system testing laboratory of the School of Engineering of the University of Seville. The method consists in several test in order to quantify the system performance:

- S-Sol: In this test, we characterize the collector array performance at high and low efficiencies and we acquire information about store heat losses
- S-Store: In this test, we characterize the store heat losses.

All the significant parameters (solar irradiation, inlet and outlet water temperature, ambient temperature and flow) have a sampling and storing frequency of 0.5 Hz. We implement a mathematical model based on a partial differential equation for the energy balance calculations. Hereinafter the insitu program [28]

The collectors array is tilted towards south at 45° and in azimuth equal to zero. The draw-offs are carried out 6 hours after solar noon for daily load volumes between 0.5 V and 1.5 V (110-140-170-200-250-300 l/day) at a hot water temperature equal to 45°C. V is the nominal tank volume in liters.

The process for obtaining the energy supplied by the solar system (Q_L), the parasitic energy (Q_{par}) and the solar fraction (f_{SOL}) according to Standard ISO 9459-5:2007 [19] is shown in Figure 4.

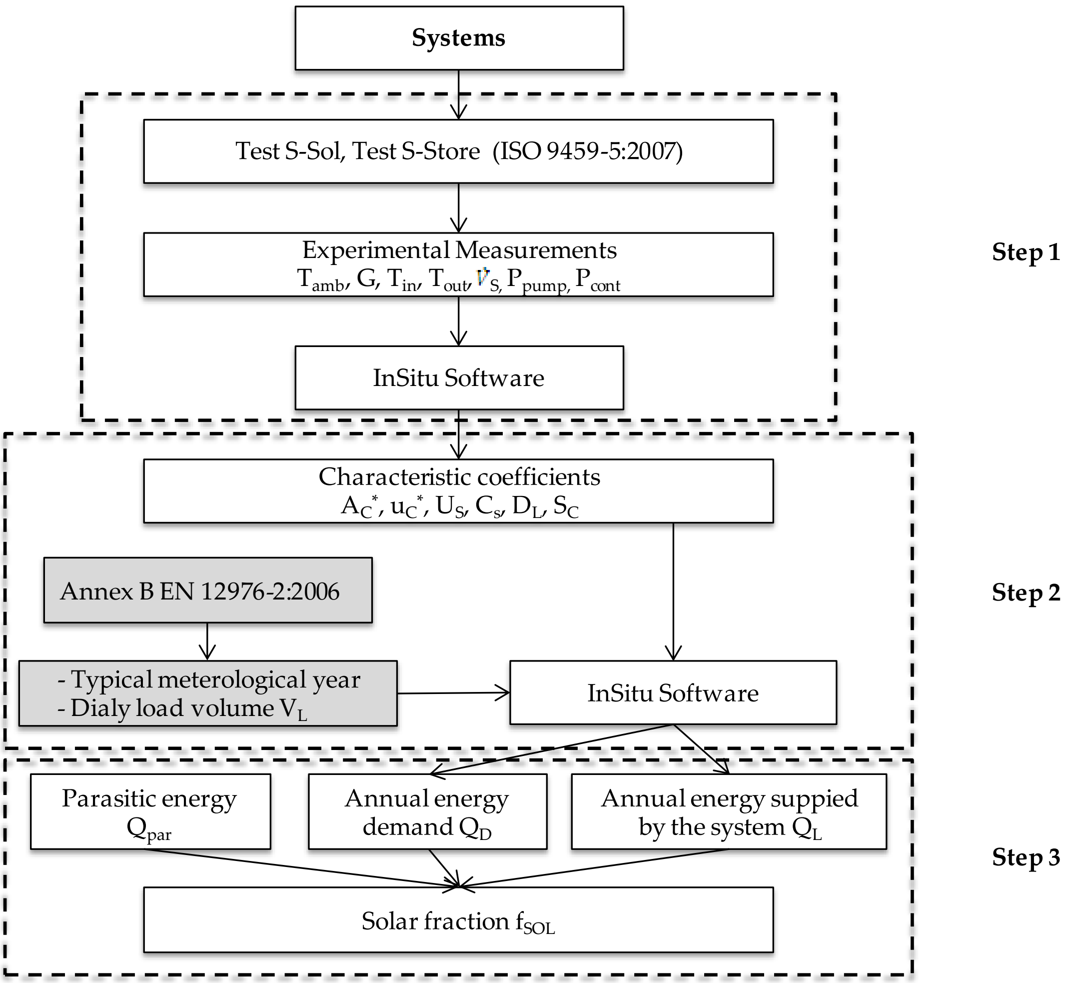

Fig 4. Process flow-diagram for the procurement of the energy supplied by the solar system and the solar fraction.

Figure 4 steps are detailed as follows:

<u>Step 1</u>: Six factory made solar heating systems have been tested thought the tests sequences S-Sol and S-Store of the Standard ISO 9459-5:2007 [19]. The measured parameters are the following:

- Ambient temperature, T_{amb}
- Irradiance on the collector plane, G
- Inlet cold-water temperature of the system T_{in}
- Outlet water temperature of the system, T_{out}
- Mass flow of consumer loop, $\dot{V}s$
- Electricity consumption of pump, P_{pump}
- Electricity consumption of controller, P_{cont}

The following indirect data are calculated from the previous measurements:

- Effective collector area, A_C*
- Effective collector loss coefficient, u_C*

- Total store heat loss coefficient, U_S
- Total store heat capacity, C_S
- Mixing constant, D_L
- Store stratification, S_C

Step2: We calculate the annual energy supplied by the solar system (Q_L) as a function of the reference locations and load volumes. The reference locations indicated in the Standard EN 12976-2:2017 [17] are Athens, Davos, Stockholm and Würzburg (Annex B). Table 2 shows the average climatic conditions of these locations.Table 2 shows the average climatic conditions of these locations.

Table 2- Reference conditions of selected locations

Locations	Annual irradiation South, 45° (kWh/m²)	Annual average outdoor air temperature (ºC)	Annual average inlet cold water temp. (ºC)
Athens	1736	18.5	17.8
Davos	1684	3.2	5.4
Würzburg	1230	9.0	10
Stockholm	1157	7.5	8.5

In this step, we also obtain the energy demand (Q_D) from the combination of the typical meteorological year of the reference locations and the user requirements (daily load volume).

The Energy parasitic (Q_{par}) is the annual electricity consumed by the pump and controller. We assume a controller operating time of 8760 h/year and 2000 h/year for the collector pump operating time.

Step 3: In the last step, we calculate the solar fraction (f_{SOL}) as a ratio between energy obtained from the solar installation to the total load requirement (equation 1). The f_{SOL} is generally used as a system performance indicator.

$$f_{SOL} = Q_{NET} / Q_D \qquad (1)$$

Where $Q_{NET} = Q_L - Q_{par}$, is the net annual energy supplied by the solar system.

3. Results and discussion

3.1.- Experimental evaluation of the long-term energy production

Following step 1 of the test methodology, we calculate the characteristic parameters: A_C*, u_C*, U_S, C_S, D_L, S_C. Table 3 shows the characteristic parameters (A_C*, u_C*, U_S, C_S, D_L, S_C) obtained from the six factory made solar heating systems according to step 1 of Figure 4.

Table 3- Characteristic parameters of the factory made solar thermal systems

System parameter	T-High-LowE	T-Low-LowE	F-LowE	T-High-Black	T-Low-Black	F-Black	Unit
A_C*	1.484	1.296	1.727	1.335	1.143	1.662	m^2
u_C*	8.123	11.79	9.74	12.45	14.36	12.83	$W/m^2·K$
U_S	2.316	2.129	2.490	2.759	3.198	2.822	W/K
C_S	0.849	0.693	0.717	0.806	0.705	0.694	MJ/K
D_L	0.023	0.076	0.043	0.026	0.050	0.032	--
S_C	0.146	0.864	0.053	0.218	0.971	0.066	--

Results can be evaluated as a function of the system parameter.

A_C*. - FSWHS (F-LowE and F-Black) have an A_C* value around 14-20% higher than high profile TSWHS (T-High-LowE and T-High-Black) and an A_C* value around 19-29% higher than low profile TSWHS (T-Low-LowE and T-Low-Black). By increasing the A_C* value, the energy production increases and improves the solar fraction. Besides all the systems have the same collector, the FSWHS present better heat removal factor of the collector loop, Fr*, leading to greater values of A_C*. An increase in the effective area of the collector (A_C*) can also be achieved by increasing the collector area or by improving the absorber treatment. For this reason, the systems tor with low absorber emissivity have A_C* values higher than systems with black painting absorber, around 4% for FSWHS, 11% for High profile TSWHS and 13% for Low profile TSWHS.

u_C*.- High profile TSWHS (T-High-LowE and T-High-Black) have an u_C*value around 3-20% lower than FSWHS (F-LowE and F-Black) and an u_C*value around 15-45% lower than low profile TSWHS (T-Low-LowE and T-Low-Black). By decreasing the u_C*value, the energy production increases and improves the solar fraction. The decrease in u_C* can be achieved by reducing the thermal losses in the collector. For this reason, systems with collector with low absorber emissivity have u_C* values lower than systems with black painting absorber, around 32% for FSWHS, 53% for High profile TSWHS and 22% for Low profile TSWHS.

U_S. - The thermal loss parameter of the collector (U_S) are similar in all systems because all TSWH have the same tank. U_S parameter depends on the construction features of the tank.

C_S.- High profile TSWHS (T-High-LowE and T-High-Black) have a C_S value around 13-15% higher than forced-circulation systems (F-LowE and F-Black) and a C_S value around 12-18% higher than low profile TSWHS (T-Low-LowE and T-Low-Black). The main cause of these differences is the absence of a reverse flow protection valve of the solar loop in High profile TSWHS.

D_L.- High profile TSWHS (T-High-LowE and T-High-Black) have a D_L value around 56-76% lower than FSWHS (F-LowE and F-Black) and a D_L value around 92-230% lower than the low profile TSWHS (T-Low-LowE and T-Low-Black). The D_L value varies depending on the pipe connection to the solar loop.

S_C. - Low profile TSWHS (T-Low-LowE and T-Low-Black) have a S_C value around 345-490% higher than high profile TSWHS (T-High-LowE and T-High-Black) and a S_C value around 1370-1530% higher than FSWHS (F-LowE and F-Black). Systems with low absorber emissivity have a S_C value around 12-49% lower than systems with black painting absorbers. The S_C parameter depends significantly on the flow of the solar loop being greater for low flows on the collector loop. . For this reason, low profile TSWHS has the highest S_C and FSWHS has the lowest S_C.

Once the characteristic coefficients have been obtained, according to step 2 of Figure 4, and with the reference conditions of Annex B of EN 12976-2:2018 [17], the annual energy supplied by the solar system (Q_L) and the annual demand energy (Q_D) can be obtained depending on the reference location and the daily load volume (V_L). The parasitic energy (Q_{par}) has been obtained according to the requirements of the Standard EN 12976-1:2018 [16]. Following the procedure described in paragraph 2.2, we calculate the solar fraction (f_{SOL}) (step 3). Tables 4 and 6 present the Q_L values as a function of the daily load volume for systems with low emissivity absorbers (T-High-LowE, T-Low-LowE and F-LowE) and systems with black painting absorbers (T-High-Black, T-Low-Black and F-Black) respectively. Figures 5 and 6 present the results graphically.

The Q_{par} value of TSWHS (T-High-LowE, T-Low-LowE) is 0 MJ. The Q_{par} value of FSWHS (F-LowE) is 213 MJ.

Table 4- Net annual energy supplied by the systems: T-High-LowE, T-Low-LowE and F-LowE

Daily load volume (l/day)	Q_{NET} (MJ)											
	Athens			Davos			Würzburg			Stockholm		
	T-High-LowE	T-Low-LowE	F-LowE	T-High-LowE	T-Low-LowE	F-LowE	T-High-LowE	T-Low-LowE	F-LowE	T-High-LowE	T-Low-LowE	F-LowE
110	4019	3992	3794	4966	4886	5026	3381	3301	3338	3326	3279	3357
140	4859	4811	4655	5770	5659	5931	4009	3891	3993	3906	3824	3987
170	5591	5495	5391	6391	6191	6613	4525	4357	4520	4376	4219	4462
200	6206	6035	5953	6813	6486	6974	4933	4674	4868	4716	4450	4728
250	6939	6680	6594	7054	6664	7154	5247	4902	5100	4936	4605	4883
300	7379	7060	6936	7096	6741	7205	5311	4998	5166	4984	4673	4930

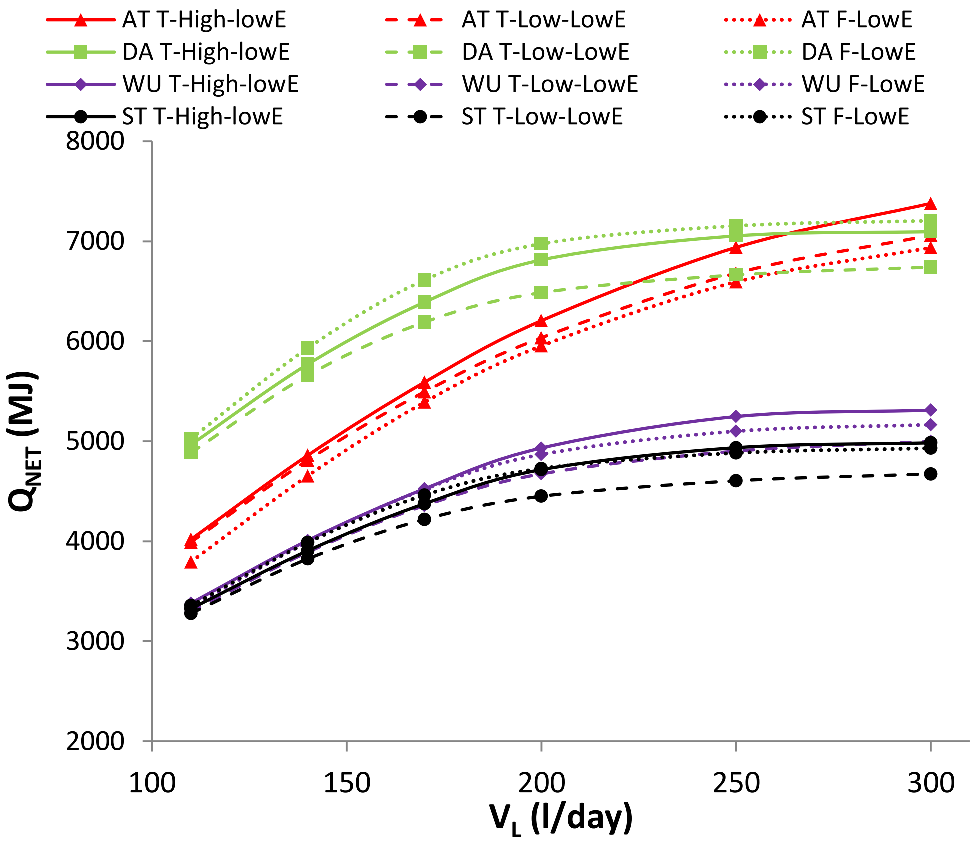

Fig 5. Net annual energy supplied by the systems T-High-LowE, T-Low-LowE and F-LowE depending on the daily load volume, for the four reference locations: AT: Athens, DA: Davos, WU: Würzburg, ST: Stockholm.

Table 4 and Figure 5 show that the solar radiation (G) and cold-water temperature (T_{main}) have the greatest influence on the net annual energy. In cold climates such as Davos, the energy production is around 3-31% higher than in warm climates such as Athens. These results can be explained because although in Davos the solar radiation and ambient temperature is slightly lower, the cold water temperature is much lower than in Athens (Table 2), encouraging the efficiency of the collector, especially at low daily load volume. For this reason, in configurations such as T-High-LowE , the net energy supplied is even higher in Athens than in Davos for high daily load volume.

Table 5 shows the influence of the daily load volume on the net annual energy for each system and location. Table 5 shows the perceptual increase of the net annual energy for each system and location, between the highest daily load volume, 300 l/day, and the last daily load volume, 100 l/day.

$$\Delta Q_{NET\ 300\text{-}110} = Q_{NET\ (300\ l/day)} - Q_{NET\ (110\ l/day)} / Q_{NET\ (110\ l/day)}\ (\%) \qquad (2)$$

Table 5- Percentage difference on net annual energy supplied by the systems for two load volumes: T-High-LowE, T-Low-LowE and F-LowE.

$\Delta Q_{NET\ 300\text{-}110}$ (%)											
Athens			Davos			Würzburg			Stockholm		
T-High-LowE	T-Low-LowE	F-LowE	T-High-LowE	T-Low-LowE	F-LowE	T-High-LowE	T-Low-LowE	F-LowE	T-High-LowE	T-Low-LowE	F-LowE
84	77	83	43	38	43	57	51	55	50	43	47

Table 5 shows that net annual energy supplied by the systems (Q_{NET}) increases around 38% and 84% by increasing the daily load volume, for four reference locations and three configurations. The influence of the daily load volume on the increase of the net energy production follows the trend of the increase of the cold-water temperature. The greatest increase of net energy production occurs in warm climates such as Athens, with an increase around 77% and 84% from low to high daily load volume. This occurs because the cold-water temperature is higher in Athens than in the rest of the locations. In Davos, there is a lower increase in the net annual energy, around 38% and 43%, since Davos has the lowest cold-water temperature. In climates with intermediate cold-water temperatures, as Würzburg and Stockholm, Net annual energy varies around 51% to 57% for Würzburg and 43% to 50% for Stockholm. This results are consistent with the efficiency curve of the systems, since as the demand increases, the average operating temperature of the collector decreases, leading to an increase of its efficiency. The increments in net annual energy are similar in the High profile TSWHS configurations with respect to FSWHS and it is slightly lower in Low profile TSWHS.

Table 4 and Figure 5 show the net annual energy produced with each configuration, FSWHS configurations supply greater net annual energy than TSWHS configurations in climates where the ambient temperature is low such as Davos and Stockholm. This is caused due to the lower thermal losses of indoor location of the storage tank in FSWHS. The increase of net annual energy supplied is low, around 2%. In climates with intermediate ambient temperatures such as Würzburg, FSWHS configurations present slightly higher net annual energy than Low profile TSWHS configurations and slightly lower net annual energy than High profile TSWHS configurations. In climates such as Athens, TSWHS configurations obtain greater net annual energy with increments of the order of 5%.

In all climates, Low Profile TSWHS configurations produce from 0.7% to 7.2% less net annual energy than High Profile TSWHS.

Table 6 and Figure 6 show the results for solar systems with black painting absorbers. In this case, the Q_{par} values of TSWHS (T-High-Black, T-Low-Black) are 0 MJ. The Q_{par} value of FSWHS (F-Black) is 209 MJ.

Table 6- Net annual energy supplied by the systems: T-High-Black, T-Low-Black and F-Black

Daily load volume (l/day)	Q_{NET} (MJ)											
	Athens			Davos			Würzburg			Stockholm		
	T-High-Black	T-Low-Black	F-Black	T-High-Black	T-Low-Black	F-Black	T-High-Black	T-Low-Black	F-Black	T-High-Black	T-Low-Black	F-Black
110	3688	3757	3591	4223	4351	4615	2978	3010	3103	2888	2953	3104
140	4450	4515	4417	4898	5022	5453	3525	3553	3714	3391	3445	3687
170	5118	5135	5091	5424	5463	6031	3982	3961	4187	3787	3786	4099
200	5656	5610	5567	5753	5682	6271	4295	4209	4443	4049	3966	4283
250	6202	6098	6030	5911	5792	6365	4473	4352	4566	4188	4064	4369
300	6412	6300	6198	5943	5830	6394	4512	4404	4602	4219	4100	4396

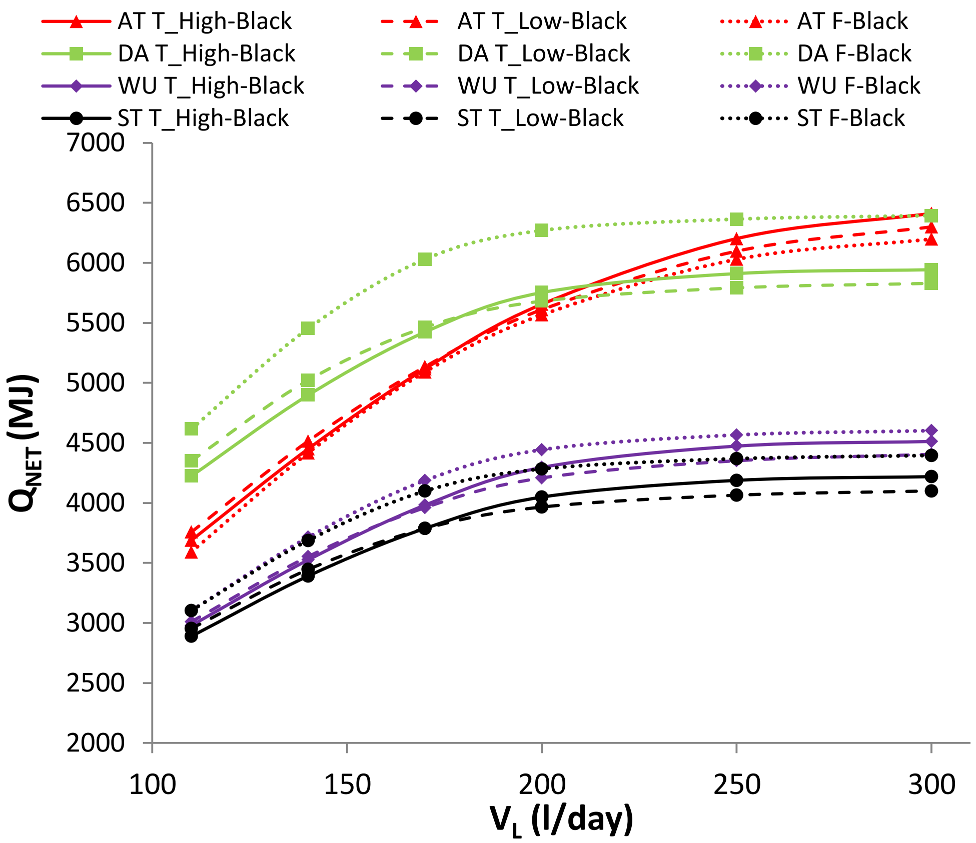

Fig 6. Net annual energy supplied by the SWHS T-High-Black, T-Low-Black and F-Black depending on the daily load volume, for four reference locations: AT: Athens, DA: Davos, WU: Würzburg, ST: Stockholm.

Table 6 and Figure 6 show again that the net annual energy obtained in Davos is higher than the net annual energy obtained in warmer climates such as Athens for all the configurations maintaining thus, the trend indicated in the previous case for low emissivity absorbers.
The net annual energy supplied also follows the previous case trend, increasing as the daily load volume increases in all the climates. In this case, the increase is smoothed (around 34% to 74%)

for the three configurations. The influence of daily load volume on the increase of net annual energy supply also follows the trend of increasing for lower cold-water temperatures.

Table 7 shows the influence of the daily load volume on the net annual energy supplied by systems with black painting absorbers.

Table 7- Percentage difference on the net annual energy supplied by the systems for two load volumes: T-High-Black, T-Low-Black and F-Black

$\Delta Q_{NET\ 300\text{-}110}$ (%)											
Athens			Davos			Würzburg			Stockholm		
T-High-Black	T-Low-Black	F-Black	T-High-Black	T-Low-Black	F-Black	T-High-Black	T-Low-Black	F-Black	T-High-Black	T-Low-Black	F-Black
74	68	73	41	34	39	52	46	48	46	39	42

Table 7 shows that the greater increase in net energy production occurs in warm climates such as Athens, with an increase around 68% to 74% mainly caused due to a higher cold-water temperature. In Davos, where the lowest cold-water temperature is found, we obtain the lower increase of net annual energy. . In climates with intermediate cold-water temperatures, as Würzburg and Stockholm, net annual energy varies around 39% to 52%. This is consistent with the efficiency curve of the system, since as the demand increases, the average operating temperature of the collector decreases, increasing its efficiency. The increments in net annual energy are similar in High profile TSWHS configurations with respect to FSWHS and it is slightly lower in Low profile TSWHS.

Table 6 and Figure 6 also show that FSWHS configurations supply greater values of net annual energy in comparison to TSWHS configurations in climates where the ambient temperature is low such as Davos and Stockholm. Differences found range from 6% to 10.4% for low profile TSWHS and from 7.7% to 11.3% for high profile TSWHS, for all load volumes, in Davos. In addition, differences around 5.1% to 8.3% respect low profile TSWHS and around 4.3% to 8.7% for high profile TSWHS, for all load volumes, in Stockholm. In climates with intermediate ambient temperatures such as Würzburg, FSWHS configuration presents higher net annual values than Low and high profile TSWHS, ranging from 3.1% to 5.7%, for low profile TSWHS and from 2.1% to 5.4% for High profile TSWHS. In warm climates such as Athens, TSWHS configurations present greater net annual energy increasing from 0.5% to 4.5% in comparison to the FSWHS configuration.

After comparing the results of net annual energy supplied by Low profile TSWHS and High Profile TSWHS with black painting absorbers, it can be seen that the differences in the net annual energy supplied between both configurations range from -3% to 3%. The results reveal that, for low daily load volumes, low profile TSWHS configuration produces slightly more energy than High Profile TSWHS configuration, for all the evaluated climates.

The influence of the absorber type of the solar collector can be observed after comparing the results of table 4 and Figure 5 with table 6 and Figure 6. Net annual energy produced by systems with low emissivity collectors is greater than in systems with black painting collectors, around 9% to 19.5% in High profile TSWHS, around 6% to 15.5% in low profile TSWHS and around 5.4% to 12.7% in FSWHS.

The solar collector efficiency has a greater impact in the net annual energy supplied by SWHS than the store heat losses effect, in climates with low inlet water temperature, very low ambient temperature and low daily load volume. Consequently, net annual energy supplied in Davos is even greater than in Athens. Athens has greater solar radiation, cold-water temperature and ambient temperature than Davos.

The store heat losses effect has a greater impact in the net annual energy supplied by SWHS than the solar collector efficiency effect, for this reason, the net annual energy supplied in Athens is greater than Davos in TSWHS configurations.

As part of knowing what percentage of the hot water annual demand is covered by each of the configurations, the solar fraction has been determined, according to eq 1.

Table 8 shows Q_D values according to the load volume and reference location calculated according Standard EN 12976-2:2017 [17] to satisfy the hot water at 45°C.

Table 8- Annual energy demand of the systems according to the daily load volume and the reference locations

Daily load volume (l/day)	Annual energy demand Q_D (MJ)			
	Athens	Davos	Würzburg	Stockholm
110	4575	6662	5888	6140
140	5823	8479	7494	7814
170	7071	10295	9099	9489
200	8319	12112	10705	11163
250	10398	15140	13381	13954
300	12478	18168	16058	16745

Table 8 shows that the energy demand decreases as the cold-water temperature increases, therefore we can observe that the energy demand is greater in Davos. Davos has around 45% more demand than the warm locations such as Athens.

Table 9 and 10 show the f_{SOL} values as a function of the daily load volume for low emissivity systems (T-High-LowE, T-Low-LowE and F-LowE) and black painting systems (T-High-Black, T-Low-Black and F-Black) respectively.
Figure 7 and 8 present the results graphically.

Table 9- Solar fraction provided by T-High-LowE, T-Low-LowE and F-LowE.

Daily load volume (l/day)	f_{SOL} : Solar fraction (%)											
	Athens			Davos			Würzburg			Stockholm		
	T_High-LowE	T-Low-LowE	F-LowE	T_High-LowE	T-Low-LowE	F-LowE	T_High-LowE	T-Low-LowE	F-LowE	T_High-LowE	T-Low-LowE	F-LowE
110	87.8	87.3	82.9	74.5	73.3	75.4	57.4	56.1	56.7	54.2	53.4	54.7
140	83.4	82.6	79.9	68.1	66.7	70.0	53.5	51.9	53.3	50.0	48.9	51.0
170	79.1	77.7	76.2	62.1	60.1	64.2	49.7	47.9	49.7	46.1	44.5	47.0
200	74.6	72.5	71.6	56.3	53.6	57.6	46.1	43.7	45.5	42.2	39.9	42.4
250	66.7	64.2	63.4	46.6	44.0	47.3	39.2	36.6	38.1	35.4	33	35.0
300	59.1	56.6	55.6	39.1	37.1	39.7	33.1	31.1	32.2	29.8	27.9	29.4

Table 10- Solar fraction provided by T-High-Black, T-Low-Black and F-Black.

Daily load volume (l/day)	f_{SOL} : Solar fraction (%)											
	Athens			Davos			Würzburg			Stockholm		
	T-High-Black	T-Low-Black	F-Black	T-High-Black	T-Low-Black	F-Black	T-High-Black	T-Low-Black	F-Black	T-High-Black	T-Low-Black	F-Black
110	80.6	82.1	78.5	63.4	65.3	69.3	50.6	51.1	52.7	47.0	48.1	50.5
140	76.4	77.5	75.8	57.8	59.2	64.3	47.0	47.4	49.6	43.4	44.1	47.2
170	72.4	72.6	72.0	52.7	53.1	58.6	43.8	43.5	46.0	39.9	39.9	43.2
200	68.0	67.4	66.9	47.5	46.9	51.8	40.1	39.3	41.5	36.3	35.5	38.4
250	59.6	58.6	58.0	39.0	38.3	42.0	33.4	32.5	34.1	30.0	29.1	31.3
300	51.4	50.5	49.7	32.7	32.1	35.2	28.1	27.4	28.7	25.2	24.5	26.3

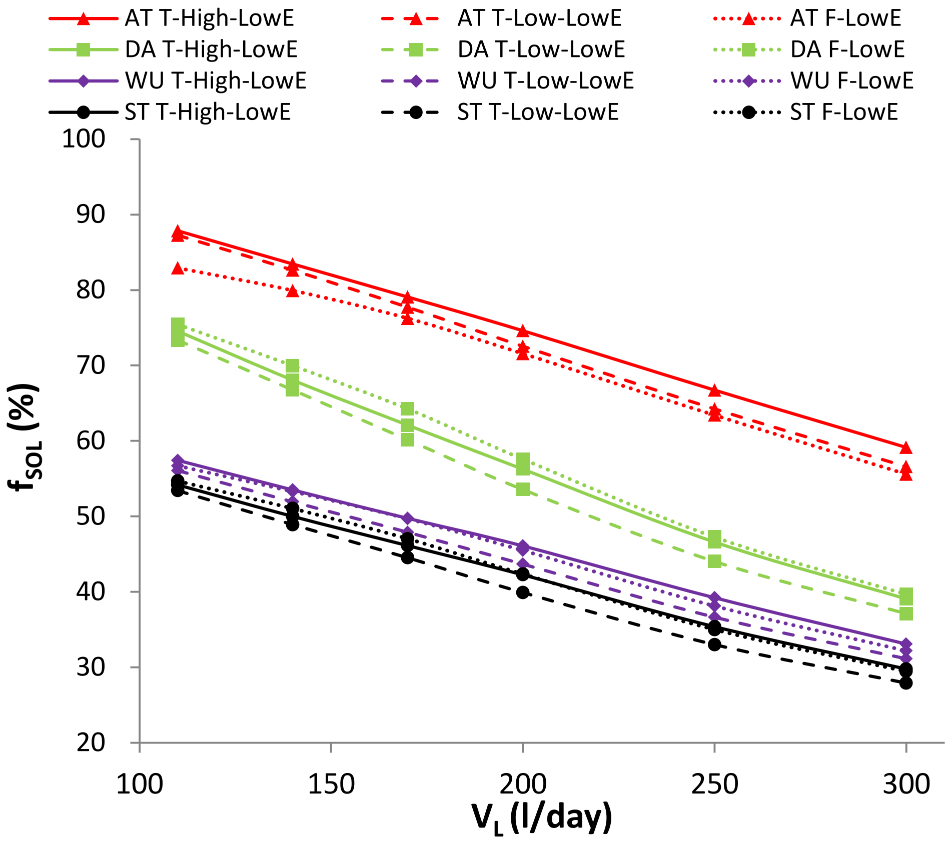

Fig 7. Solar fraction of T-High-LowE, T-Low-LowE and F-LowE systems depending on the daily load volume, for four reference locations: AT: Athens, DA: Davos, WU: Würzburg, ST: Stockholm.

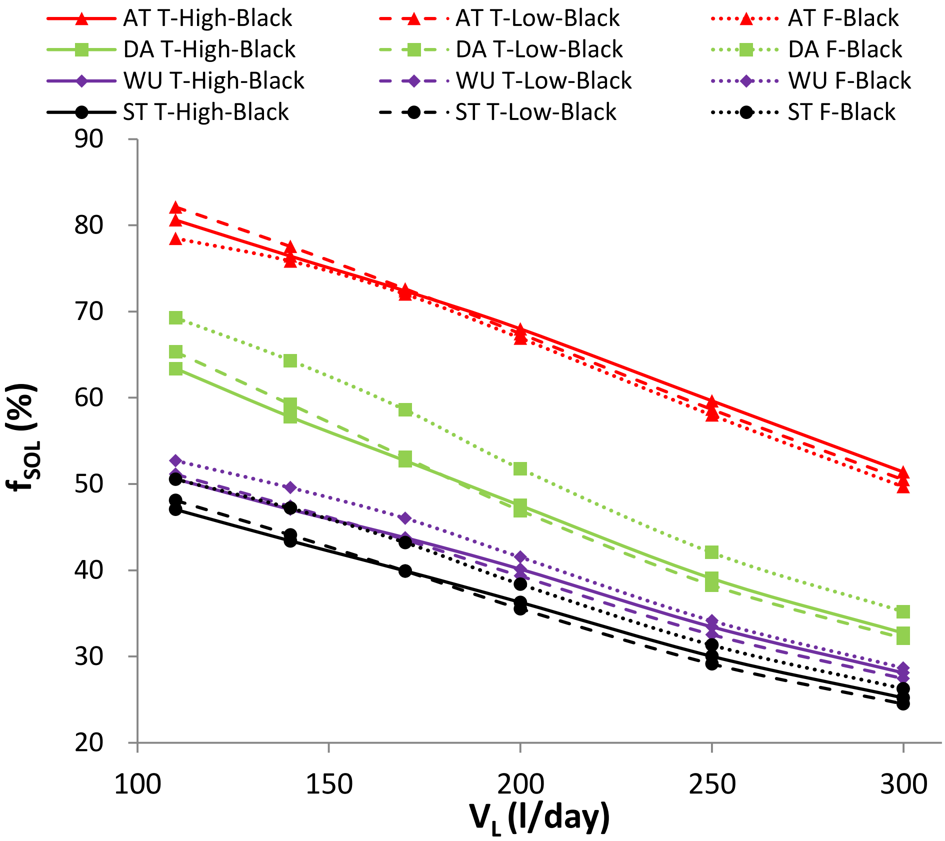

Fig 8. Solar fraction of T-High-Black, T-Low-Black and F-Black depending on the daily load volume, for four reference locations: AT: Athens, DA: Davos, WU: Würzburg, ST: Stockholm.

The highest values of the solar fraction occur in Athens location, followed by Davos, Würzburg and finally Stockholm, for all configurations and collector´s types. This is logical because Athens is the location with the highest solar radiation (table 2) and the lowest annual energy demand (table 8).

Davos is the location where more net annual energy is produced (table 4 and 6), but Athens is the location where the solar fraction is higher (table 9 and 10), for all configurations and collector´s types. This is caused due to a greater energy demand (Q_D) in Davos than in Athens (around 45%) (Table 8), meanwhile, the percentage increase in the net annual energy supply in Davos with respect to Athens is much lower (less than 25%)

3.2.- Techno-economic analysis

In order to analyze the energy cost of the tested solar systems, we compare the LCOE obtained for the different daily load volumes and reference locations. The LCOE is evaluated according to the equation 4 in which the numerator considers the expenses that take place throughout all the useful life of the installation and the denominator considers the energy generated over the same period [29]. The variables r and s of this expression represent the average rate of consumer price index and the average energy price, both of them highly dependent on the country examined:

$$LCOE = \left[C_I + \sum_{t=i_i}^{i_f} \frac{C_{OMt}}{(1+r)^t} + \frac{C_R}{(1+r)^{15}} \right] \Bigg/ \left[\sum_{t=i_i}^{i_f} \frac{E_{IPt}}{(1+s)^t} \right] \quad (4)$$

Table 11 shows the investment costs (C_I) of the solar systems tested. These values have been supplied by the manufacturer.

Table 11- Costs of the systems, without VAT, with a nominal volume of 200 liters depending on the system type

Components	System costs C_I (€)					
	T-High-LowE	T-Low-LowE	F-LowE	T-High-Black	T-Low-Black	F-Black
Tank of 200 liters	750	750	750	750	750	750
Selective collector plane 2.58 m^2	658	658	658	0	0	0
Blank painting collector plane 2.58 m^2	0	0	0	500	500	500
Antifreeze fluid (2 liters)	15	15	15	15	15	15
Long connection pipe	45	43	310	45	43	310
Short connection pipe	15	25	310	15	25	310
Supporting frame	320	225	200	320	225	200
Expansion vessel 8 L	0	39	39	0	39	39
Security valves	29	29	29	29	29	29
Reverse flow protection valve of consumer loop.	10	10	10	10	10	10
Thermosiphonic valve	0	39	29	0	39	29
Drain valve	0	21	21	0	21	21
Manometer	0	12	12	0	12	12
Pump	0	0	155	0	0	155
Controller	0	0	180	0	0	180
Rest of Kit system	39	47	172	39	47	172
TOTAL	1881	1913	2890	1723	1755	2732

For the same type collector, the total cost differences in high and low profile TSWHS are very insignificant, being 1.7% for selective collectors and 1.8% for black painting collectors. This occurs mainly because high profile TSWHS have a high structure cost. Low profile TSWHS have an overall higher cost because they require auxiliary equipment such as expansion vessel and thermosiphonic valve. However, the cost differences between TSWHS are more significant depending on the quality of the absorber, being around of 9% for both high profile systems and low profile systems.

In the calculation of LCOE parameter, the following assumptions have been made:

- Useful life (t) equal to 25 years.

- Annual Operations and Maintenance costs (C_{OM}) equal to 0.02% of the investment cost.
- Assembly cost for all systems equal to 350€ on thermosiphon systems and 500€ on forced-circulation systems, included in the investment cost.
- Electricity cost equal to 0.12 c€/kWh from the first year.
- Replacement cost (C_R) are equal to zero.
- Average rate of consumer price index (r) is equal to 2%.
- Average rate of energy price (s) is equal to 1.4%.

Table 12- System costs per collector surface unit, system and assembly costs per collector surface unit and collector costs per collector surface unit

	T-High-LowE	T-Low-LowE	F-LowE	T-High-Black	T-Low-Black	F-Black
System costs (€/m^2)	729	741	1120	668	680	1059
System and assembly costs (€/m^2)	845	858	1314	784	797	1253
Collector costs (€/m^2)	255	255	255	194	194	194

The costs of high and low profile TSWHS per collector surface unit is very similar, with differences around 2%. However, the cost per collector surface unit of FSWHS is around 55% higher than for TSWHS configurations.

According to table 12, the cost of the solar collector with low emissivity absorber and black painting absorber is 255 €/m^2 and 194 €/m^2 respectively. These costs are in line with those indicated by Maurer [8] of 240 €/m^2. The solar collector cost represents around 22% to 30% compared to system and assembly costs for TSWHS and around 15% to 19% for FSWHS. The system and assembly costs in FSWHS configurations are around 51% to 56% more expensive than in TSWHS configurations.

As the costs of BIST depend on each application and therefore can be very variable, hence, a comparison with SWHS is not advisable.

Table 13 and 14 show LCOE values obtained for low emissivity systems (T-High-LowE, T-Low-LowE and F-LowE) and black painting systems (T-High-Black, T-Low-Black and F-Black) respectively.

Table 13- LCOE for SWHS T-High-LowE, T-Low-LowE and F-LowE

Daily load volume (l/day)	LCOE (c€/MJ)											
	Athens			Davos			Würzburg			Stockholm		
	T_High-LowE	T-Low-LowE	F-LowE	T_High-LowE	T-Low-LowE	F-LowE	T_High-LowE	T-Low-LowE	F-LowE	T_High-LowE	T-Low-LowE	F-LowE
110	3.68	3.76	6.14	2.98	3.07	4.64	4.38	4.55	6.98	4.45	4.58	6.94
140	3.04	3.12	5.01	2.56	2.65	3.93	3.69	3.86	5.84	3.79	3.92	5.85
170	2.65	2.73	4.32	2.31	2.42	3.52	3.27	3.44	5.16	3.38	3.56	5.22
200	2.38	2.49	3.91	2.17	2.31	3.34	3.00	3.21	4.79	3.14	3.37	4.93
250	2.13	2.25	3.53	2.10	2.25	3.26	2.82	3.06	4.57	3.00	3.26	4.77
300	2	2.13	3.36	2.08	2.23	3.23	2.79	3.00	4.51	2.97	3.21	4.73

Table 14- LCOE for SWHS T-High-Black, T-Low-Black and F-Black

Daily load volume (l/day)	LCOE (c€/MJ)											
	Athens			Davos			Würzburg			Stockholm		
	T-High-Black	T-Low-Black	F-Black	T-High-Black	T-Low-Black	F-Black	T-High-Black	T-Low-Black	F-Black	T-High-Black	T-Low-Black	F-Black
110	3.73	3.71	6.20	3.25	3.21	4.82	4.62	4.64	7.17	4.76	4.73	7.17
140	3.09	3.09	5.04	2.81	2.78	4.08	3.90	3.93	5.99	4.05	4.05	6.04
170	2.69	2.72	4.37	2.53	2.55	3.69	3.45	3.52	5.32	3.63	3.69	5.43
200	2.43	2.49	4.00	2.39	2.46	3.55	3.20	3.32	5.01	3.39	3.52	5.20
250	2.22	2.29	3.69	2.33	2.41	3.50	3.07	3.21	4.87	3.28	3.43	5.09
300	2.14	2.22	3.59	2.31	2.39	3.48	3.05	3.17	4.84	3.26	3.40	5.06

Table 13 and 14 show that the system efficiency is higher for locations with very low cold-water temperatures. For this reason, Davos has lower LCOE values despite having lower solar radiation than Athens for low daily load volumes. The influence of cold-water temperature in LCOE improvement decreases as daily load volume increases. This occurs because LCOE values in Athens are lower than in Davos for high daily load volumes.

The maximum LCOE value reached in all systems is found in the FSWHS. In general, LCOE values in SWHS with low emissivity absorber are higher than SWHS with black painting absorber. The LCOE of T-Low-LowE system is slightly higher than T_High-LowE system in all reference locations and daily load volumes. The LCOE difference between both systems is slightly higher when increasing the daily load volume. The smallest difference in the LCOE for both systems is obtained in locations with high annual solar irradiation values of such as Athens and Davos. The greater differences in the LCOE are found in locations with low annual irradiation, such as Würzburg and Stockholm, with differences around 1.72-2.60 c€/MJ.LCOE values of F-LowE systems are higher than in other systems with low emissivity collector.

Table 13 shows that the LCOE values of T-Low-Black systems are practically similar to the LCOE values of T-High-Black systems in all reference locations. The maximum LCOE differences in

TSWHS with black painting absorbers are found in locations with the lower solar radiation values such as Würzburg and Stockholm reaching values of about 4.6%.

LCOE values of F-Black systems are higher than the other systems with black painting collector. The greater differences of LCOE are found for low annual irradiation locations, such as Würzburg and Stockholm, with differences around 1.79-2.55 c€/MJ.

The maximum LCOE differences between two types of TSWHS are reached when increasing the daily load volume well above the nominal volume. The maximum LCOE differences reached is 9% in TSWHS with selective absorbers and low annual irradiation climates.
The maximum LCOE difference between the two types of SWHS, thermosiphon and forced-circulation system is 68%, found for climates with high annual solar irradiation and ambient temperature such as Athens and for low daily load volumes (110 l/day).

4. - Conclusions

It has been shown that the daily load volume has significant influence on the net annual energy supplied particularly in warm weather locations. The net annual energy varies around 38% to 88% between low and high daily load volume. The greater the cold-water temperature, the greater the influence of the daily load volume on the net annual energy supplied. The daily load volume is the parameter with the greatest influence on the net annual energy. Therefore, in terms of net annual energy and in climates such as Athens, it is advisable to design the systems with a daily load volume lower than the storage tank volume daily, since in that case, the energy efficiency of the solar system would be improved. In cold climates such as Davos, the increase in energy production produced by a variation in the daily load volume is much lower.

The net annual energy in cold or temperate climates is greater in FSWHS configurations. Net annual energy in warm climates is greater in TSWHS configurations. However, the increase in energy production of FSWHS respect to TSWHS in cold or temperate climates (maximum values around 9.5% for very cold climates and low daily load volume) is much lower than the increase in their costs (around 50%). Therefore, LCOE values of FSWHS configurations can be around 68% higher than TSWHS.

In TSWHS, High profile TSWHS normally produces more net annual energy than Low Profile TSWHS but the difference is insignificant, reaching maximum values around 3.9% especially for high daily load volumes and low absorber emissivity. For low daily load volumes, Low Profile TSWHS produces more net annual energy than High Profile TSWHS especially in cold climates, low daily load volumes and black painting absorber. These values can reach around 0.5-3%.

In all the studied cases, LCOE for TSWHS is lower than for FSWHS configurations. Low profile TSWHS present very similar costs and performance than high profile TSWHS, especially for daily load volumes below the nominal tank volume, collectors with black painting absorber and locations with high irradiation. The differences would be significant when comparing a high profile system with a low profile system but with different quality of the collector absorber.

Therefore, factory made low profiles TSWHS are a good technical and economic alternative for a better architectural integration of traditional high profile TSWHS.

FSWHS represents an economic alternative if the economic inputs derived from its use as an element of the building exceed around 50% the costs of the TSWHS.

References

[1] Shady Attia, Polyvios Eleftheriou, Flouris Xeni, Rodolphe Morlot, Christophe Ménézo, Vasilis Kostopoulos, Maria Betsi, Iakovos Kalaitzoglou, Lorenzo Pagliano, Maurizio Cellura, Manuela Almeida, Marco Ferreira, Tudor Baracu, Viorel Badescu, Ruxandra Crutescu, Juan Maria Hidalgo-Betanzos. Overview and future challenges of nearly zero energy buildings (nZEB) design in Southern Europe. Energy and Buildings. Volume 155, 2017, Pages 439-458. https://doi.org/10.1016/j.enbuild.2017.09.043.

[2] Annual Energy Outlook 2017 with projections to 2050. January 5, 2017. U.S. Energy Information Administration. https://www.eia.gov/outlooks/aeo/pdf/0383(2017).pdf (Access on line on 8th february 2018)

[3] Dario Traum, Luiza Demoro, Kyle Harrison, Ethan Zindler. Global Climatescope 2017.The Clean Energy Country Competitiveness Index. Bloomberg New Energy Finance. http://global-climatescope.org/en/download/insights/climatescope-2017-clean-energy-investment.pdf

[4] Directive 2010/31/EU of the European Parliament and of the Council of 19 May 2010 on the energy performance of buildings. http://eur-lex.europa.eu/legal-content/EN/TXT/?uri=CELEX:32010L0031.

[5] Directive (EU) 2018/844 of the European Parliament and of the Council of 30 May 2018 https://eur-lex.europa.eu/eli/dir/2018/844/oj.

[6] Directive 2012/27/EU of the European Parliament and of the Council of 25 October 2012 on energy efficiency. http://data.europa.eu/eli/dir/2012/27/oj.

[7] Chr. Lamnatou, J.D. Mondol, D. Chemisana, C. Maurer. Modelling and simulation of Building-Integrated solar thermal systems: Behaviour of the coupled building/system configuration. Renewable and Sustainable Energy Reviews. Volume 48. 2015. Pages 178-191. https://doi.org/10.1016/j.rser.2015.03.075.

[8] Christoph Maurer, Christoph Cappel, Tilmann E. Kuhn. Progress in building-integrated solar thermal systems. Solar Energy. Volume 154, 2017, Pages 158-186. https://doi.org/10.1016/j.solener.2017.05.065.

[9] IEA, Solar heating and cooling programme. Task 56 “Building Integrated Solar Envelope Systems for HVAC and Lighting. http://task56.iea-shc.org/publications. (26/07/2018).

[10] Christoph Maurer, Christoph Cappel, Tilmann E. Kuhn. Simple models for building-integrated solar thermal systems. Energy and Buildings. Volume 103. 2015, Pages 118-123. https://doi.org/10.1016/j.enbuild.2015.05.047

[11] Li Li , Ming Qu, Steve Peng. Performance evaluation of building integrated solar thermal shading system: Active solar energy usage. Renewable Energy, 109 (2017). Pages 576-585 http://dx.doi.org/10.1016/j.renene.2017.03.069.

[12] Sun, Xiao-Yu & Sun, Xiao-Dan & Li, Xin-Gang & Wang, Zhen-Qing & He, Jian & Wang, Bin-Sheng. (2014). Performance and building integration of all-ceramic solar collectors. Energy and Buildings. 75. 176–180. https://doi.org/10.1016/j.enbuild.2014.01.045

[13] Yuguo Yang, Qichun Wang, Dapeng Xiu, Zhibin Zhao, Qizheng Sun. A building integrated solar collector: All-ceramic solar collector. Energy and Buildings, Volume 62, July 2013, Pages 15-17. https://doi.org/10.1016/j.enbuild.2013.03.002.

[14] Zhang X, Shen J, Tang L, Yang T, Xia L, et al. (2015) Building Integrated Solar Thermal (BIST) Technologies and Their Applications: A Review of Structural Design and Architectural Integration. J Fundam Renewable Energy Appl 5: 182. doi:10.4172/20904541.1000182

[15] http://www.domasolar.com. (Access on line 30th July)

[16] European Standard EN 12976-1:2017, Thermal solar systems and components. Factory made systems. Part 1: General Requeriments.

[17] European Standard EN 12976-2:2017, Thermal solar systems and components. Factory made systems –Part 2: Test methods.

[18] International Standard ISO 9459-2:2008, Solar heating – Domestic water heating Systems. Part 1: Outdoor test methods for system performance characterization and yearly performance prediction of solar-only systems.

[19] International Standard ISO 9459-5:2007, Solar heating – Domestic water heating Systems. Part 5: System performance characterization by means of whole-system tests and computer simulation.

[20] ICC 900/SRCC 300:2015, Solar Thermal System Standard

[21] Abel S. Vieira, Rodney A. Stewart, Roberto Lamberts, Cara D. Beal. Residential solar water heaters in Brisbane, Australia: Key performance parameters and indicators. Renewable Energy, Volume 116, Part A. 2018, Pages 120-132. https://doi.org/10.1016/j.renene.2017.09.054.

[22] Kok Seng Ong, Kevin Osmond, Wei Li Tong; Reverse flow in natural convection heat pipe solar water heater, International Journal of Low-Carbon Technologies, Volume 10, Issue 4, 1 December 2015, Pages 430–437, https://doi.org/10.1093/ijlct/ctu017.

[23] G.L. Morrison, J.E. Braun. System modelling and operation characteristics of thermosiphon solar water heaters. Solar Energy, 34 (1985), pp. 389-405.

[24] Soteris A. Kalogirou. Flat-plate collector construction and system configuration to optimize the thermosiphonic effect. Renewable Energy. Volume 67. 2014. Pages 202-206. https://doi.org/10.1016/j.renene.2013.11.021.

[25] Bo Carlsson, Michaela Meir, John Rekstad, Dieter Preiß, Thomas Ramschak.Replacing traditional materials with polymeric materials in solar thermosiphon systems – Case study on pros and cons based on a total cost accounting approach. Solar Energy. Volume 125. 2016. Pages 294-306. https://doi.org/10.1016/j.solener.2015.12.005.

[26] SOLE S.A. Solar Appliances Manufacturer. https://www.eurostar-solar.com/solar-water-heaters.html.

[27] CHROMAGEN. http://chromagen.com/209430. (access on line on 8th March 2017)

[28] InSitu Scientific Software. Dynamic System Testing Program (Version 2.7). ISS, Kriegerstr. 23 d, D-82110 Germering. FRG, 1996.

[29] P. Konstatin, Praxisbuch Energiewirtschaft: Energieumwandlung, ´transport und -beschaffung im liberalisierten Markt, Springer. Berlin, 2009.

Nomenclature

A_C^* (m^2) → Effective collector loop area

C_I (€) → Investment costs

C_{OMt} (€) → Annual operations and Maintenance costs

C_R (€) → Replacement cost

C_S (MJ/K) → Total store heat capacity

D_L (−) → Draw-off mixing parameter

f_{SOL} (−) → Solar fraction

G (W/m^2) → Irradiance on the collector plane.

LCOE (c€/MJ) → Levelised cost of energy

Q_D (MJ) → Annual energy demand

Q_L (MJ) → Energy supplied by the solar system

Q_{NET} (MJ) → Net annual energy supplied by the solar system

r (−) → Average rate of consumer price index

s (−) → Average rate of energy price

S_C (−) → Collector loop stratification parameter

T_{amb} (ºC) → Ambient temperature

T_{in} (ºC) → Inlet water temperature of consumer loop

T_{out} (ºC) → Oulet water temperature of consumer loop

u_C^* (W/m^2K) → Effective collector loss coefficient

U_S (W/K) → Total store heat loss coefficient

U_S (W/K) → Total store heat loss coefficient

V (l) → Tank nominal volume

V_L (l/day) → Daily load volume

$\dot{V}s$ (l/h) → Flow of consumer loop